Two Kinds of Calcium Channels in Canine Atrial Cells

Differences in Kinetics, Selectivity, and Pharmacology

BRUCE P. BEAN

From the Department of Physiology and Biophysics, The University of Iowa, Iowa City, Iowa 52242

ABSTRACT Currents through Ca channels were recorded in single canine atrial cells using whole-cell recording with patch pipettes. Two components of Ca channel current could be distinguished. One ("I_{fast}") was present only if cells were held at negative potentials, was most prominent for relatively small depolarizations, and inactivated within tens of milliseconds. The other ("I_{slow}"), corresponding to the Ca current previously reported in single cardiac cells, persisted even at relatively positive holding potentials, required stronger depolarizations for maximal current, and inactivated much more slowly. Both currents were unaffected by tetrodotoxin and both were reduced by Co. I_{fast} had the same size and kinetics when Ca was exchanged for Ba, while I_{slow} was bigger and slower with Ba as the charge carrier. In isotonic $BaCl_2$, fluctuation analysis showed that I_{fast} had a smaller single channel current than I_{slow}. I_{slow} was much more sensitive to block by nitrendipine than was I_{fast}; also, I_{slow}, but not I_{fast}, was increased by the dihydropyridine drug BAY K8644. Isoproterenol produced large increases in I_{slow} but had no effect on I_{fast}.

INTRODUCTION

Ca-selective channels in the surface membrane of heart cells are important for electrical activity, for excitation-contraction coupling, and for helping mediate neurotransmitter modulation of the heartbeat. It has long been clear that cardiac Ca channels may differ from some kinds of Ca channels found in various noncardiac cells, such as neurons and egg cells (see Hagiwara and Byerly, 1981; Hagiwara, 1983; Tsien, 1983; Reuter, 1984). However, it has usually been assumed that cardiac cells have a single class of Ca channels (but see Lee et al. [1984] for a recent challenge). In contrast, there is well-established evidence for considerable diversity of Ca channels in noncardiac cells (Hagiwara, 1983). Especially striking are the descriptions of two kinds of Ca channels occurring in

Address reprint requests to Dr. Bruce P. Bean, Dept. of Neurobiology, Harvard Medical School, 25 Shattuck St., Boston, MA 02115.

J. GEN. PHYSIOL. © The Rockefeller University Press · 0022-1295/85/07/0001/30$1.00

Volume 86 July 1985 1–30

single cells, such as starfish eggs (Hagiwara et al., 1975), polychaete eggs (Fox and Krasne, 1984), and the ciliate *Stylonychia* (Deitmer, 1984).

In neurons, too, evidence has mounted for the existence of at least two different kinds of Ca channels that may be present in the same cell. From action potential recordings, Llinas and Yarom (1981*a*, *b*) found evidence for two components of Ca current in guinea pig inferior olivary neurons: a current elicited only from hyperpolarized cells that activates at relatively negative membrane potentials and inactivates quickly, and a current that requires more depolarized potentials for activation and inactivates slowly.

Recently, whole-cell voltage-clamp recordings from chick and rat sensory neurons in culture have revealed two distinct components of Ca channel current having just these characteristics (Nowycky et al., 1984*a*; Carbone and Lux, 1984*a*; Fedulova et al., 1985), and single channel recordings (Carbone and Lux, 1984*b*; Nowycky et al., 1984*b*) leave no doubt that the currents arise from two kinds of Ca channels with different conductances. Evidence for the co-existence of two kinds of Ca channels in one cell has also come from recent whole-cell recordings from cultured anterior pituitary (Matteson and Armstrong, 1984*a*; Armstrong and Matteson, 1985; Cohen and McCarthy, 1985) and neuroblastoma (Tsunoo et al., 1984, 1985; Yoshii et al., 1985) cells.

I have found evidence that atrial cells dissociated from dog hearts also have two distinct kinds of Ca channels. One kind of channel, which has not been previously described in heart cells, appears to be similar to the low-depolarization–activated channel in neurons: it is present only if cells are held negative to −50 mV, produces a maximal current at −30 mV in physiological Ca, and inactivates quickly. The other channel is like that previously described in ventricular cells: it requires stronger depolarizations for activation, inactivates slowly, and inactivates only with steady holding potentials positive to −30 mV. The two kinds of channels have different degrees of discrimination between Ca and Ba and different single channel conductances. The channels also have different sensitivities to dihydropyridine drugs, and only the slowly inactivating channel is regulated by β-adrenergic receptor stimulation.

A preliminary report of this work has appeared (Bean, 1985).

METHODS

Isolation of Cells

Hearts were removed from mongrel dogs and placed into ice-cold Tyrode's solution composed of (mM): 150 NaCl, 4 KCl, 2 $CaCl_2$, 2 $MgCl_2$, 10 glucose, and 10 HEPES, pH 7.40. Usually, dogs were anesthetized with Nembutal and the hearts were beating, but in some cases, the hearts had also been stopped by KCl injection. There was no obvious difference in the properties of the cells isolated from stopped hearts. A chunk of tissue ~5 mm^2 was cut from the right atrial appendage and minced with scissors in nominally 0-Ca Tyrode's (same as above but with no added $CaCl_2$). The tissue pieces were transferred to an enzyme solution containing 0.6 mg/ml collagenase (type I; Sigma Chemical Co., St. Louis, MO) and 0.05 mg/ml protease (Sigma type VII) in 0-Ca Tyrode's, incubated at 37°C with gentle stirring, and triturated with a broken-off Pasteur pipette about every 30 min. The procedure was adapted from that of Bustamente et al. (1982) for human

cells, except that type I collagenase gave better results than type V. After a reasonable number of dissociated cells appeared in the solution, at times ranging from 30 min to 3 h for different hearts, the solution was passed through 200-μm nylon mesh and spun at ~1,000 rpm for 4 min. The pellet was resuspended in 0.5 mM Ca Tyrode's solution. Cells were kept at room temperature and used within 15 h. (Some cells remained viable for several days, but day-old cells showed shifts in the current-voltage relations for both Ca currents of ~20 mV in the hyperpolarizing direction.) Only cells that were relaxed, striated, and rod-shaped in 2–10 mM Ca Tyrode's were used.

Voltage Clamp

Whole-cell currents were recorded following the procedure of Hamill et al. (1981). Cells were placed in the chamber, rinsed with Tyrode's solution containing 2–10 mM Ca, and approached with fire-polished pipettes containing the internal solution of (mM): 120 CsCl, 10 Cs_2EGTA, 5 $MgCl_2$, and 10 HEPES, adjusted to 7.45 with CsOH. After a gigaseal was formed and the patch was ruptured to give a whole-cell clamp, currents were allowed to stabilize for several minutes and the external solution was changed to the Na-free recording solution. This was either an isotonic $BaCl_2$ solution (110 mM $BaCl_2$ and 10 mM HEPES, pH adjusted to 7.40 with BaOH, called "115 mM Ba" solution) or tetraethylammonium (TEA)-Tyrode's solution with added divalents (5–20 mM $CaCl_2$ or $BaCl_2$, 154 mM TEA Cl, 2 mM $MgCl_2$, 10 mM glucose, and 10 mM HEPES, pH adusted to 7.40 with TEA-OH).

Cell Capacity and Series Resistance

The parallel combination of cell resistance and seal resistance was typically 2–10 GΩ. The average cell capacity was 70 ± 3 pF (mean ± SEM, N = 71). The series resistance of the pipette (measured as the time constant of the uncompensated capacity transient divided by cell capacity) was usually two to four times that of the unsealed pipette (0.7–2.5 MΩ), as has been remarked for other preparations (Marty and Neher, 1983; Dubinsky and Oxford, 1984; Matteson and Armstrong, 1984*b*; Corey et al., 1984). 60–80% of the measured series resistance could be compensated for before the transient began to ring. In the absence of series resistance compensation, the decay of the capacity transient could be fit extremely well by a single exponential (Fig. 1). After compensation, the average time constant of the capacity transient was 94 ± 5 μs (N = 30), and the residual, uncompensated series resistance was 1.6 ± 0.03 MΩ. Since the Ca channel currents were almost always <2 nA, even in 115 mM Ba, series resistance errors were small. Sometimes the capacity transient gradually slowed as the experiment progressed; this was prevented or reduced in most experiments by the steady application of mild suction (~20 in. of water), which had no obvious effect on Ca currents or cell survival.

Analysis of Ca Channel Currents

The ionic conditions were chosen to isolate currents through Ca channels and no other time- or voltage-dependent currents were obvious (with the exception of the apparent outward Cs flow through Na channels discussed in Results). Inward Na current was eliminated by substitution of TEA for Na, Ca flow through Na channels was blocked by the 10 μM TTX present when Ca was used as the charge carrier, K currents were eliminated by the internal Cs and external TEA or Ba, and possible Ca-activated currents were eliminated by 10 mM EGTA in the internal solution. Ca channel currents were elicited by depolarizations given every 3–15 s, passed through an eight-pole low-pass Bessel filter with a corner frequency set at 0.5–5 kHz, digitized at 20–400-μs intervals, and stored and analyzed on a laboratory computer. Leak and capacity currents were

subtracted using scaled current from signal-averaged small pulses that elicited no ionic current. The capacity and leak currents were sometimes fit by a smooth exponential plus a steady current so that no extra noise would be introduced by scaling of the leak sweep (in some cases, two exponentials plus a steady current were needed for highly accurate fitting after series resistance compensation). In most of the currents displayed in the figures, the first few milliseconds (usually 2–2.4 ms) after the voltage step have been omitted in order to truncate the spike of outward current (see Fig. 6). Peak Ca channel currents were read as the average of five points around the peak. Experiments were done at 22°C.

Ensemble Fluctuation Analysis

Ensembles of currents were generated by a series of identical voltage pulses (usually ~100) delivered every 2 or 3 s. Currents were filtered at 2 kHz (−3 dB, eight-pole Bessel). Variance was calculated in a pairwise manner; difference currents for two successive

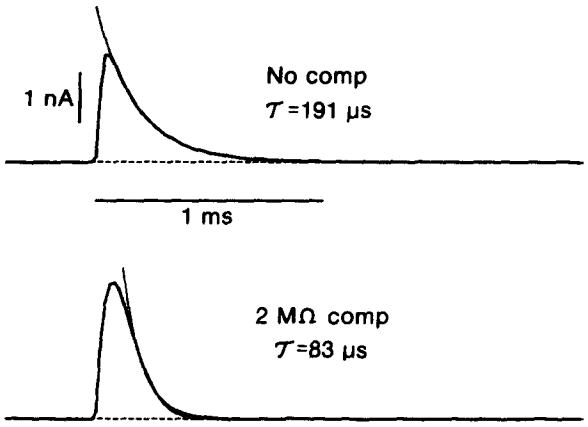

FIGURE 1. Time course of capacity transient for a 10-mV step depolarization from −80 mV. The pipette resistance before sealing was 1.5 MΩ; the input resistance after sealing was 4 GΩ. The total cell capacity was 51 pF. Exponentials are best (least-squares) fits to falling phase of current between 60 and 10% of its peak value. 5-kHz filter. 115 mM Ba external solution. Cell B27B.

sweeps were squared and divided by two, and the results were averaged over all the pairs. This procedure minimized errors arising from steady rundown of currents, which was in any case very slow for depolarizations up to 0 mV (typically, <2% for a series of 100 currents), where currents were small, and still only 0–10% for a series of 100 depolarizations to +30 or +40 mV, where currents were large. Even with 10% drift during the ensemble, artifactual variance from rundown would be <1% of the total variance seen at these potentials.

The variance during the period of depolarization was corrected for background variance by subtracting the variance at the holding potential, calculated from the same ensemble of sweeps (using the initial segment of holding current preceding the onset of the depolarization). This correction procedure assumes that background (non-Ca channel) variance does not depend on membrane potential or membrane conductance, in contrast to the situation encountered in voltage-clamp studies of the node of Ranvier, where the background variance of the system does change significantly with membrane conductance (see Conti et al., 1976; Sigworth, 1980). In the case of the whole-cell clamp with gigaseal

pipettes, the assumption that background variance does not change with membrane conductance appears to be a good approximation. Three theoretical and experimental considerations support this idea. First, for realistic values of pipette series resistance, cell conductance, and cell capacitance, it is expected that the predominant source of nonchannel noise will be the cell capacitance in series with the pipette resistance (see Marty and Neher, 1983). Even at the peak of the Ca channel current, the membrane conductance (typically <20 nS) would produce nonchannel noise of only ~0.3 pA^2 or less, measured with a 0–2-kHz bandwidth (see Hamill et al., 1981); this can be compared with typical experimental background noise of 7–25 pA^2. Second, experiments with electrode-cell models composed of resistors and capacitors support this view: a network composed of a 3.3-MΩ "electrode" and a 68-pF, 1-GΩ "cell" had a variance of 12.98 pA^2 with series resistance compensation in the clamp set at 2.6 MΩ (2-kHz filter). The variance increased to only 13.16 pA^2 when the "cell" resistance was decreased to 50 MΩ. Finally, in an experiment on a real cell, the variance at the Ca channel reversal potential was found to be equal to the background variance at the holding potential, despite the large difference in conductance (unpublished experiment on a cultured rat ventricular cell with M. C. Nowycky and R. W. Tsien).

Single channel current was estimated by plotting background-corrected variance as a function of mean current and fitting a theoretical curve drawn according to variance = $iI - I^2/N$ (Sigworth, 1980). Usually, the curve was the best (least-squares) fit to the data; however, records arising from the subtraction procedure used to derive data for the fast current in isolation tended to have considerable scatter near the origin (see Fig. 12) and in these cases fits were made by eye, giving more weight to data points for the larger current levels.

The calibration of the computer program was checked in two ways: by analyzing an ensemble of mock data generated by a computer simulation, and by analyzing a series of records from a single channel recording (filtered at 1 kHz). In both cases, the analysis yielded values of i within 20% of the actual single channel current.

The extraction of single channel current estimates from the fluctuation data depends on the assumption that the fast channels and slow channels each form a population of identical channels that gate independently of one another (see Sigworth, 1980). How rigorously the assumptions are met remains uncertain. Even if all slow channels are identical and independently gated, complicated switching between different modes of gating may occur (Hess et al., 1984), and if channels entered different modes for times that were long compared with the time scale of the variance calculations (comparing sweeps a few seconds apart), the population would be effectively inhomogeneous. However, any such errors must be small in the case of slow channels since both the size and voltage dependence of single channel currents estimated by fluctuation analysis are similar to those from direct single channel recording.

Application to Drugs

When drugs were applied (or ion substitution experiments were carried out), both control and drug solutions were run through the chamber (~1 ml) at rates of 5–15 ml/min. Nitrendipine (the kind gift of Dr. Alexander Scriabine, Miles Laboratories, Inc., New Haven, CT) was made up daily as a 5-mM stock in ethanol and stored in the dark. The application of 0.6% ethanol alone (three times the concentration present when 10-μM nitrendipine solutions were made) had no effect on I_{fast} and reduced I_{slow} by 15%. Isoproterenol was made daily as a 1-mM stock in 5 mM ascorbate and 5 mM HEPES, pH 7.4, and was applied to cells within 10 min of breaking the cell membrane and beginning dialysis, as its effectiveness in modulating I_{slow} decreased in cells dialyzed for more than ~20 min.

RESULTS

Two Components of Current

Fig. 2 shows whole-cell currents from a cell bathed in a 115 mM Ba solution containing 10 μM tetrodotoxin (TTX). Panel *A* shows currents elicited by various depolarizations from two different holding potentials. With the cell held at −80

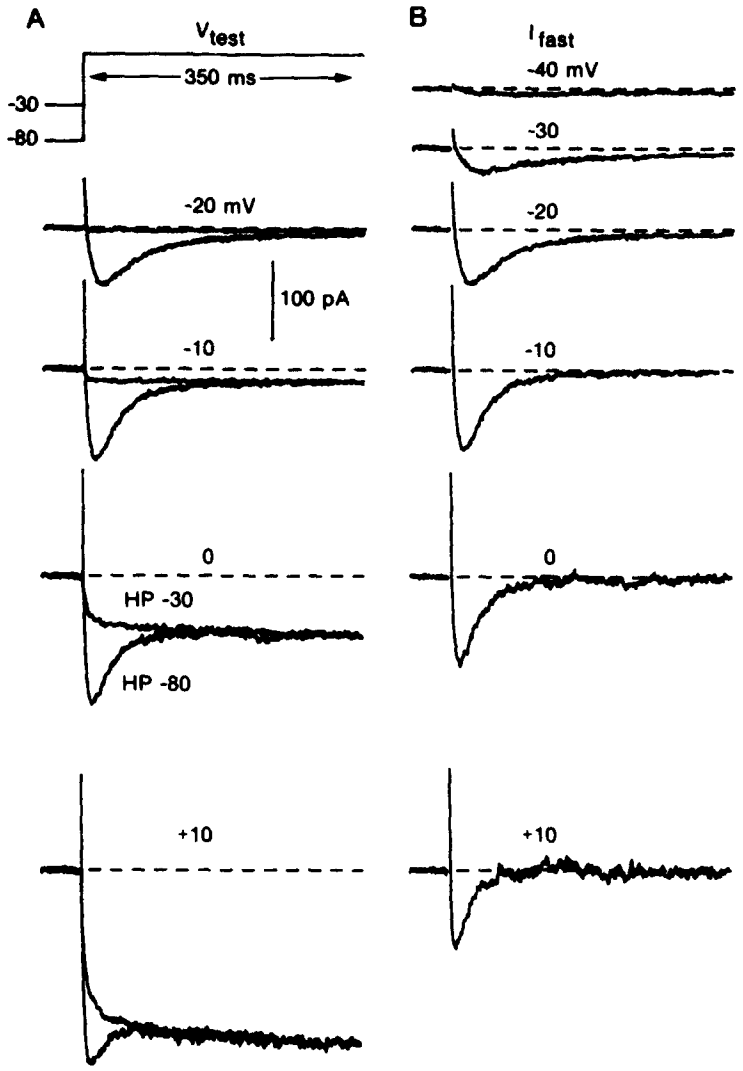

FIGURE 2. Two components of Ba current. 115 mM Ba, 10 μM TTX. (*A*) Currents elicited by steps from −80 or −30 mV; for −30 traces, the holding potential (HP) was changed to −30 for 2 s before test pulse depolarization. Traces shown are averages of three to six sweeps, leak and capacity corrected. (*B*) Difference currents from traces in *A*, along with current elicited by steps to −40 and −30 from −80 mV (leak and capacity corrected). 0.5-kHz filter. Cell capacity, 69 pF. Cell B28C.

mV, a step to −20 mV elicits an inward current that reaches a peak in ~20 ms and then decays smoothly with a half-time of ~20 ms. However, with the cell held at −30 mV, the step to −20 mV fails to elicit a significant current. For larger steps from −80 mV, the inward current reaches a peak in 10–15 ms and then decays to a nearly steady inward current, which becomes larger with increasing depolarization. Steps from −30 mV fail to elicit the early peak current but instead produce a current that rises smoothly and, after 50–200 ms, superimposes with the steady current elicited from −80 mV.

These results can be explained simply if steps from −80 mV elicit two distinct components of current: one that activates and then inactivates fairly quickly and is completely inactivated by holding at −30 mV, and one that activates more slowly to a steady value and is unchanged when elicited from −30 mV. The results in the rest of the paper support this interpretation and suggest that the two components of current arise from two distinct populations of Ca channels with different properties.

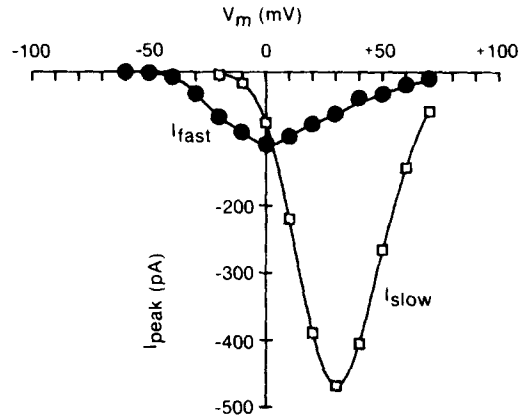

FIGURE 3. Peak current-voltage relations for two components of current in 115 mM Ba. Same cell as in Fig. 2.

On this interpretation, the current due to the component that rapidly activates and inactivates ("I_{fast}") can be separated from the slower, maintained component ("I_{slow}") simply by subtracting the current elicited from −30 mV from that elicited from −80 mV. Fig. 2*B* shows I_{fast} isolated in this way. Current first begins to be elicited at about −40 mV, and with larger depolarizations becomes larger, activates more quickly, and inactivates more quickly. Peak current is largest at 0 mV; for larger depolarizations, peak current begins to decline, while both activation and inactivation continue to get faster.

Fig. 3 compares the peak current-voltage relations for the two components of current; I_{fast} was isolated by subtraction, as in Fig. 2, and I_{slow} was elicited in isolated form by steps from −30 mV. I_{slow} requires larger depolarizations for significant activation but continues to increase up to +30 mV, where it is much larger than the I_{fast} component.

These results were typical of 33 atrial cells studied in 115 mM Ba. Every cell

had both components of current, clearly separable by holding potential, but there was considerable variation in the relative magnitude of the two components. Peak I_{fast} varied from 30 to 400 pA (mean 118 ± 15 pA) and peak I_{slow} varied from 250 to 2,700 pA (mean 1,139 ± 100 pA). In cells isolated from the right ventricle, I_{fast} was either very small or missing entirely, and I_{slow} was considerably larger than in atrial cells. Of five ventricular cells studied by the protocol in Fig. 2, with the same solutions, three had no detectable I_{fast} (<5 pA), while the other two had peak I_{fast} values of 10 and 20 pA; I_{slow} was 2,000–4,000 pA. When I_{fast} was present in ventricular cells, it had kinetics and voltage dependence similar to those in atrial cells.

Both components of current in atrial cells were also seen with bathing solutions

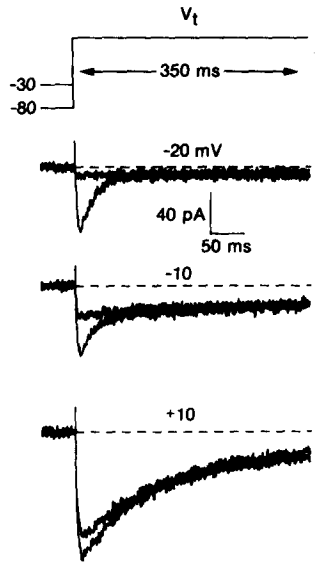

FIGURE 4. Two components of Ca current. 5 mM Ca TEA, 10 μM TTX. Currents are single sweeps, leak and capacity corrected, filtered at 0.5 kHz. Cell capacity, 53 pF. Cell B23C.

containing 5 mM Ca, the physiological Ca concentration for a dog. Fig. 4 shows that the two components of Ca current can be separated by holding potential, as for the Ba currents in Fig. 2. With Ca as the charge carrier, however, the two components both activate fairly quickly. The distinction between them is most obvious for small depolarizations, where the component elicited from a holding potential of −30 mV does not inactivate significantly during the pulse. At more depolarized potentials, where the current elicited from −30 does begin to inactivate substantially, the presence of two different components would not be obvious were it not for the guidance of the results at low depolarizations and with Ba as the charge carrier.

Fig. 5 shows the peak current-voltage relations for isolated I_{fast} and I_{slow} in 5 mM Ca. As suggested by a comparison of Figs. 5 and 3, it was generally true that

the magnitudes of I_{fast} and I_{slow} were less different in 5 mM Ca than in 115 mM Ba. For the cell in Fig. 5 in 5 mM Ca, peak I_{fast} was 54 pA (−30 mV) and peak I_{slow} was 102 pA (+20 mV), a ratio of 1:2. With the same cell in 115 mM Ba, peak I_{fast} was 142 pA (0 mV) and peak I_{slow} was 635 pA (+30 mV), a ratio of 1:4. In other cells, comparisons of equal concentrations of Ca and Ba suggest that at least part of the difference in the I_{fast}:I_{slow} ratio is due to ion species (see Fig. 9), but an additional dependence on ion concentration is not ruled out. For six cells studied in 5 mM Ca, peak I_{fast} was 24 ± 7 pA and peak I_{slow} was 103 ± 21 pA.

Effects of TTX

Could I_{fast} actually represent Ca or Ba flowing through Na channels rather than Ca channels? Although 10–20 μM TTX was normally present in the external

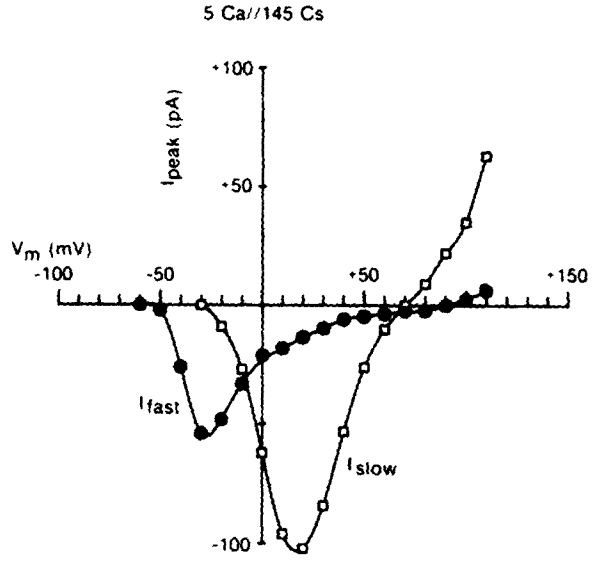

FIGURE 5. Peak current-voltage relations for currents in 5 mM Ca. Same cell as in Fig. 4.

solution, mammalian cardiac Na channels have a low affinity for TTX ($K_d \approx 1$ μM; cf. Cohen et al., 1981) and the cells have a large number of Na channels (I_{Na} >5 nA in 150 mM Na). The experiment in Fig. 6 tested the possibility that I_{fast} is carried through Na channels; current elicited by a step from −80 to −20 in 115 mM Ba (predominantly I_{fast}) was recorded before and after the addition of 10 μM TTX. TTX produces no change in peak inward current or in its decay; instead, it partially blocks a very rapid outward current that precedes I_{fast}. A reasonable interpretation is that the outward current results from outward Cs flow through Na channels. Some of this outward current always remained unblocked in 10 or 20 μM TTX; the unblocked portion probably represents Cs flux through a fraction of unblocked Na channels and (perhaps) gating current from Na channels. Consistent with this explanation is the observation that the outward current could be almost totally eliminated by holding positive to −50

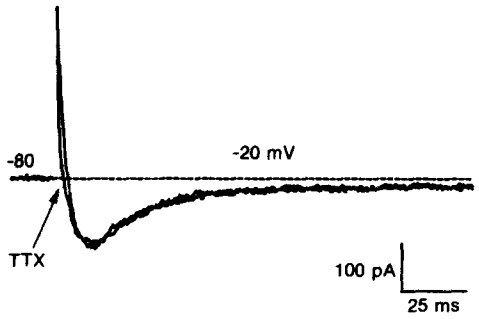

FIGURE 6. Lack of effect of TTX on fast component. 115 mM Ba external solution. Currents were recorded before and 1.5 min after superfusion with 10 μM TTX-containing solution. Leak and capacity corrected. Cell capacity, 85 pF. Cell 29B.

mV. Even in the absence of TTX, the outward current is over by the time of peak I_{fast} and the experiment leaves little doubt that I_{fast} is not through Na channels. With Ba solutions, the TTX-inhibitable current was outward at all potentials. In 20 mM Ca solutions, the TTX-blockable current was a very rapid inward current at −40 to −30 mV and outward positive to −30 mV, which is consistent with a small Ca permeability through the Na channel. In studies of I_{fast}, 10 or 20 μM TTX was always present in Ca solutions, while it was sometimes omitted from Ba solutions if high flow rates (and large volumes) were needed.

Block by Co

To further test the hypothesis that both I_{fast} and I_{slow} represent Ca channel current, I examined the ability of Co to block the currents. Fig. 7 shows that Co blocked both I_{fast} and I_{slow} to a similar degree. 2 mM Co blocked I_{fast} measured at −10 mV to 43% of control (229 to 102 pA) and I_{slow} measured at +30 mV to 37% of control (2,316 to 887 pA). These results were typical; in applications to three cells bathed in 115 μM Ba, 2 mM Co blocked I_{fast} at −10 mV to 37 ± 2%

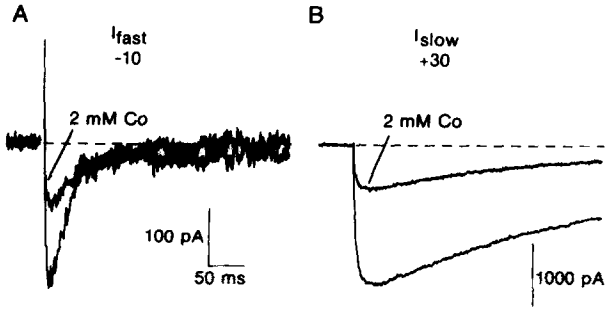

FIGURE 7. Inhibition of I_{fast} and I_{slow} components by 2 mM Co. Left: effect of Co on I_{fast} (isolated by subtraction as in Fig. 2), leak and capacity corrected. Right (same application): effect on I_{slow} (leak- and capacity-corrected current for −30 to +30 mV depolarization). 115 mM Ba, 10 μM TTX. 0.5-kHz filter. Cell capacity, 125 pF. Cell B21A.

and I_{slow} at +30 mV to 39 ± 5%. These results are consistent with the interpretation that both I_{fast} and I_{slow} are Ca channel currents.

Voltage Dependence of Inactivation

The experiments in Figs. 2 and 4 suggest that I_{fast} is available at a holding potential of −80 mV but is completely inactivated at −30 mV. Fig. 8 shows the voltage dependence of I_{fast} inactivation in more detail and contrasts it with the

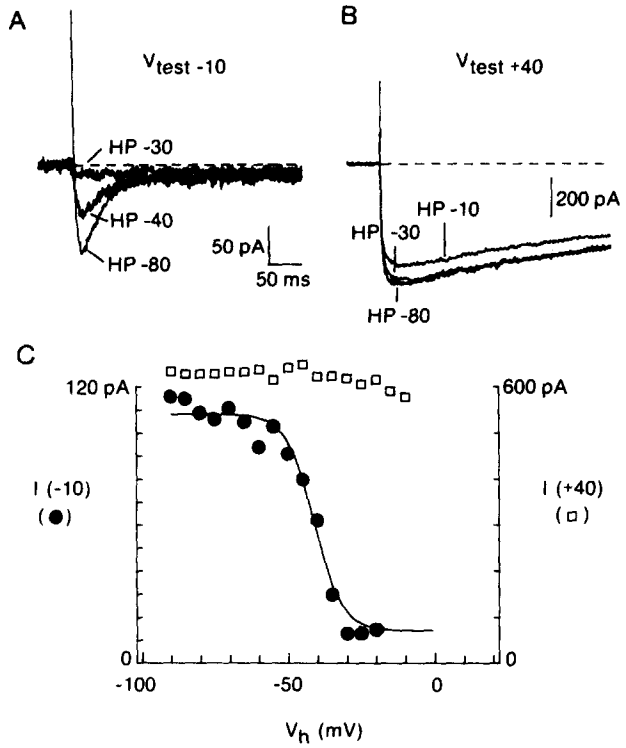

FIGURE 8. Inactivation of I_{fast} and I_{slow} with holding potential. External solution 115 mM Ba, 10 μM TTX. Different holding potentials were established for 2 s before test pulse; currents are leak and capacity corrected and filtered at 0.5 kHz. In *A*, current from −80 mV is average of four sweeps. The solid line in *C* is drawn according to $I = I_{max}/[1 + \exp(V_h - V_K)/k] + I_{con}$, with I_{max} = 94 pA, V_K = −41 mV, k = 4.8, I_{con} = 14 pA. Cell B28C.

behavior of I_{slow}. Current elicited by test pulses to −10 mV (predominantly, but not exclusively, I_{fast}) is nearly maximal for holding potentials negative to −60 mV and is reduced to about half at a holding potential of −40 mV. The current elicited from −30 mV is only a small nonactivating current (I_{slow} in the present interpretation). The closed circles in Fig. 8*C* show peak current at −10 mV as a function of holding potential. The points can be fit well by a Hodgkin-Huxley-like equation plus a constant. A simple interpretation of the curve is that I_{fast} inactivates with a Hodgkin-Huxley-like voltage dependence and is totally inac-

tivated at a holding potential of −30 mV, leaving only I_{slow}, which does not inactivate significantly between −30 and −20 mV.

Fig. 8*B* shows, in contrast, the effect of holding potential on current elicited by pulses to +40 mV. At this test potential, there is very little effect of changing holding potential between −80 and −30 mV. Only a very small fraction of current is inactivated at −30 mV, which is consistent with the small size of I_{fast} at similar test potentials in other experiments (see Fig. 3). I_{slow} is not inactivated at all at −30 mV, as judged by the superposition at late times of the currents from −30 and −80 mV; even at −10 mV, it shows only slight inactivation despite the fact that steady current begins to be activated at the −10-mV holding potential (see panel *A*). Even holding at +20 mV for 2 s, which activates large I_{slow} currents, fails to produce much inactivation in 115 mM Ba solutions, which is consistent with the lack of much decay of current at these potentials (see Fig. 2).

The results in Fig. 8 were typical: in three experiments in 115 mM Ba, the inactivation curve for I_{fast} had a midpoint of −45 ± 3 mV and a slope factor of 5.2 ± 1.2, and I_{slow} showed very little inactivation up to +20 mV. A series of experiments in 20 mM Ca gave a similar clear separation of the voltage dependence of inactivation for the two currents, except that steady state inactivation of I_{slow} was more prominent than in 115 mM Ba, and currents were completely inactivated by holding at +10 mV for 2 s. In four cells in 20 mM Ca, the midpoint for I_{fast} was −53 ± 3 mV, with a slope factor of 4.9, while the midpoint for I_{slow} was −10 ± 2 mV, with a slope factor of 5.2 mV. In some cells in 20 mM Ca, test pulses were used that gave currents composed of sizeable fractions of both I_{fast} and I_{slow}; these produced inactivation curves with two components, one with a midpoint near −50 mV and one with a midpoint near −10 mV. All of these results are most easily explained by the hypothesis of two populations of channels with very different inactivation properties; it would be difficult to explain the results as reflecting a single population of channels unless arbitrarily complicated kinetic properties are invoked.

In one cell, inactivation of I_{fast} was compared with inactivation of I_{Na}. The inactivation curve for I_{fast} (measured in 20 mM Ca TEA with 10 μM TTX) had a midpoint at −49 mV (slope factor 6.9), while the inactivation curve for I_{Na} (measured in 20 mM Ca TEA with 20 mM NaCl added and no TTX) had a midpoint at −62 mV (slope factor 4.9). (In the same cell, I_{slow} had an inactivation curve with a midpoint of −1 mV and a slope factor of 4.5.) A physiologically important aspect of this result is that at some potentials, I_{Na} may be inactivated, while I_{fast} is still available (see Discussion).

Comparison of Ca and Ba Currents

As already noted, changing the bathing solution from 5 mM Ca to 115 mM Ba increased peak I_{slow} much more than peak I_{fast}. Fig. 9 shows results that explicitly compare currents in 20 mM Ca with those carried by 20 mM Ba. Changing the ion species has strikingly little effect on I_{fast}. Both the size and kinetics of I_{fast} at −10 mV are almost precisely the same in both solutions, and, as the peak current-voltage relation in Fig. 9*C* shows, there was little change in peak current at any potential. This suggests that Ca and Ba are about equally permeant through the

fast Ca channel. In contrast, I_{slow} was profoundly changed by substituting Ba for Ca. Currents elicited by test pulses from 0 to +40 mV were larger with Ba as the charge carrier; positive to +50 mV, currents in Ba were smaller and the reversal potential for current was consistently less positive in 20 mM Ba (+75 ± 7 mV, two cells) than in 20 mM Ca (more than +90, three cells). The increase in the peak of the *I-V* curve in 20 mM Ba suggests that Ba can carry more current than Ca through the slow Ca channel. It would be difficult to be completely sure

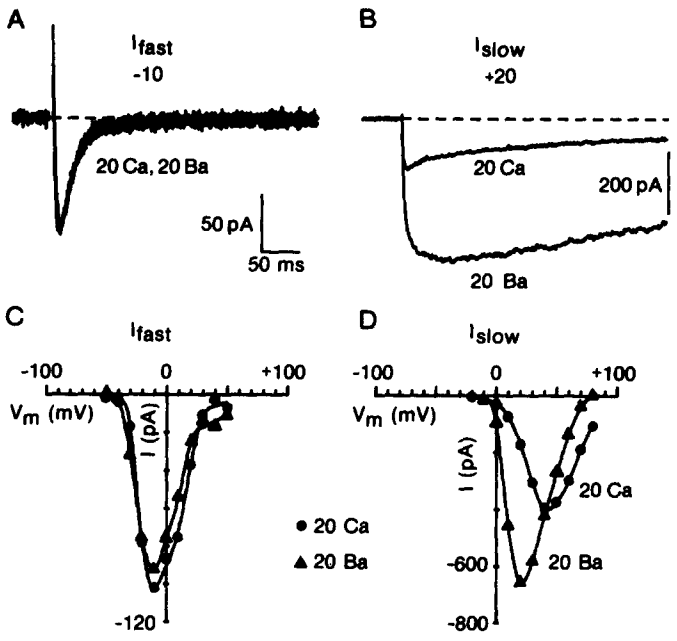

FIGURE 9. Currents carried by Ca and Ba. Currents in *A* and *B* labeled "20 Ba" were recorded 5 min after changing 20 mM Ca TEA, 10 μM TTX solution to 20 mM Ba TEA, 10 μM TTX. (*A*) I_{fast} isolated by subtraction as in Fig. 2. Each trace used in the subtraction was the average of three to six sweeps. (*B*) I_{slow} elicited by pulse from −30 to +20 mV. Single sweeps, leak and capacity corrected. 0.5-kHz filter. (*C*) Peak current-voltage relation for I_{fast} in 20 mM Ca and 20 mM Ba. Values in 20 mM Ca were obtained ~5 min before changing to 20 mM Ba; current at −10 mV had run down by ~10% by the time the current shown in *A* was recorded, just before solution change. (*A*) Peak current-voltage relation for I_{slow} elicited from −30 mV. Cell B29C.

about this point from Fig. 9*D* alone because of possible changes in the fraction of channels opened at various potentials in Ca and Ba solutions. However, nonstationary fluctuation analysis of current through slow Ca channels in cultured rat ventricular cells confirms that the single channel current carried by 10 mM Ba (0.14 ± 0.01 pA at 0 mV) is considerably larger than in 10 mM Ca (0.08 ± 0.005 pA) at the same potential (unpublished experiments with M. C. Nowycky and R. W. Tsien). A similar difference has been reported in bullfrog ventricular cells (Hess and Tsien, 1984). The larger current carried by Ba ions in the slow

channel can be reconciled with the more negative reversal potential by a model of ion permeation that invokes two divalent ion-binding sites in the channel and different affinities for Ca and Ba (Hess and Tsien, 1984; Almers and McCleskey, 1984).

Although I_{fast} at −10 mV had the same kinetics in Ba as in Ca, the kinetics of I_{slow} were very different in Ba and Ca: there was much less decay in Ba, and peak current was much later (Fig. 9*B*). Fig. 10 shows that the lack of effect of ion species on inactivation kinetics was seen at all potentials for I_{fast}, and that inactivation was much faster in 20 mM Ca than in 20 mM Ba for I_{slow} positive to +0 mV (below this potential, inactivation even in 20 mM Ca was slow or absent, as in Fig. 4).

Fluctuation Analysis

To test more directly the possibility that the ion permeation properties of the

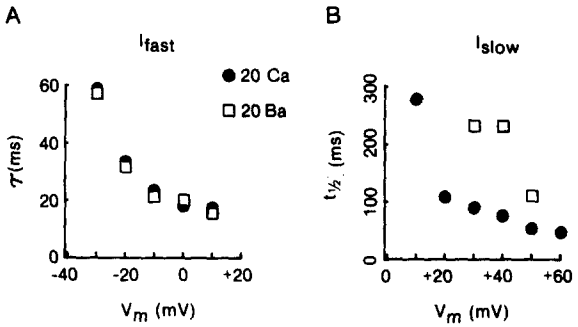

FIGURE 10. Rates of inactivation in 20 mM Ca or 20 mM Ba. (*A*) Time constant for decay of I_{fast}. Smooth currents were obtained by signal-averaging three to eight sweeps elicited from −30 mV and subtracting these from an equal number elicited from −80 mV. The falling phase of resulting I_{fast} was fit with a least-squares exponential; fits were excellent at all potentials. (*B*) Decay of I_{slow} in Ca and Ba. The decay of I_{slow} is nonexponential and the rate of decay was therefore quantitated by the half-time. Cell B29A.

two channels are different, the nonstationary fluctuation analysis technique developed by Sigworth (1980) was used to estimate the single channel current for each of the two kinds of channels. As shown previously (Fenwick et al., 1982; Hagiwara and Ohmori, 1982), the technique is well suited for whole-cell voltage-clamp recordings because of the low background conductance (and low background noise) and the small number of channels (and large current fluctuations). The external solution was 115 mM Ba, chosen in hopes of maximizing single channel current. Fig. 11 shows results from an experiment that estimated the single channel current for each component of current at −10 mV in the same cell. A series of 124 identical pulses from −80 to −10 mV was applied, and the mean and variance for the current at each time point in the trace were calculated from the resulting currents. Then, a series of 97 pulses from −40 to −10 mV was applied, and the variance and mean were calculated in an identical way. As expected, the mean current elicited from −80 mV showed both components of

current, while the fast-inactivating portion was lacking in the series from −40 mV. Similarly, the variance of the ensemble elicited from −80 mV showed two components, with an early peak that was missing from the variance derived from the ensemble elicited from −40 mV; at later times during the depolarization, the variances derived from the two ensembles coincided, as did the mean currents.

If the extra transient of variance from a holding potential of −80 mV does in fact arise from channels different from those remaining active at −40 mV, it can be isolated from the total variance by subtraction of the two records, exactly as the fast component of current is isolated by subtraction, since variances arising from independent sources are additive. Thus, both the variance and mean current arising from the fast-inactivating component can be obtained in isolation. Similarly, on this interpretation, the variance and current remaining at the −40 mV holding potential represent a single population of I_{slow} channels. In Fig. 12,

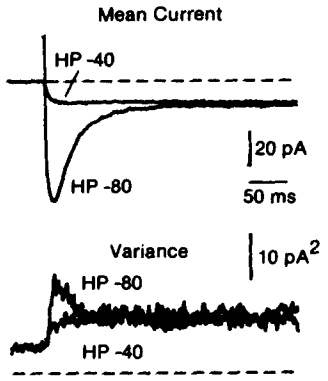

FIGURE 11. Mean current and variance for ensembles of currents elicited from −40 or −80 mV. Ensembles were generated by a series of identical pulses to −10 mV (124 for the series from −80, 97 for the series from −40) delivered at 1 pulse/2 s. Mean currents were leak and capacity corrected. Dashed lines show zero-current and zero-variance levels. The variance trace was smoothed by averaging over five points around each time point. 115 mM Ba, 10 μM TTX. 46 pF. Cell B22G.

this procedure is used to estimate the single channel current for each of the populations of channels. In Fig. 12, *A* and *B*, the variance and current from I_{slow}, the current elicited from −40 mV, are compared, and the variance vs. current relation is fit with the relationship expected for a population of N identical channels that gate independently of one another:

$$\text{variance} = iI - I^2/N,$$

where I is the mean current and i is the single channel current (Sigworth, 1980). The variance-mean relationship is approximately linear; this indicates that the maximal probability of channel opening during the depolarization (p_{max}) is low, since the theoretical relationship (which can be recast as variance = $Np[1 - p]i^2$) predicts a noticeably parabolic relationship for p_{max} of approximately >0.2. The low value of p_{max} is expected, since −10 mV is just on the foot of the I_{slow} *I-V* curve in 115 mM Ba (Fig. 3). The fit of the theory to the experimental points in

Fig. 12*B* gives a value of i for I_{slow} of 0.53 pA. (The theoretical line in Fig. 12*B* is drawn with $N = 19{,}200$ channels, but any $N > 300$ would give a practically indistinguishable curve.)

The same procedure is carried through in Fig. 12, *C* and *D*, for the mean

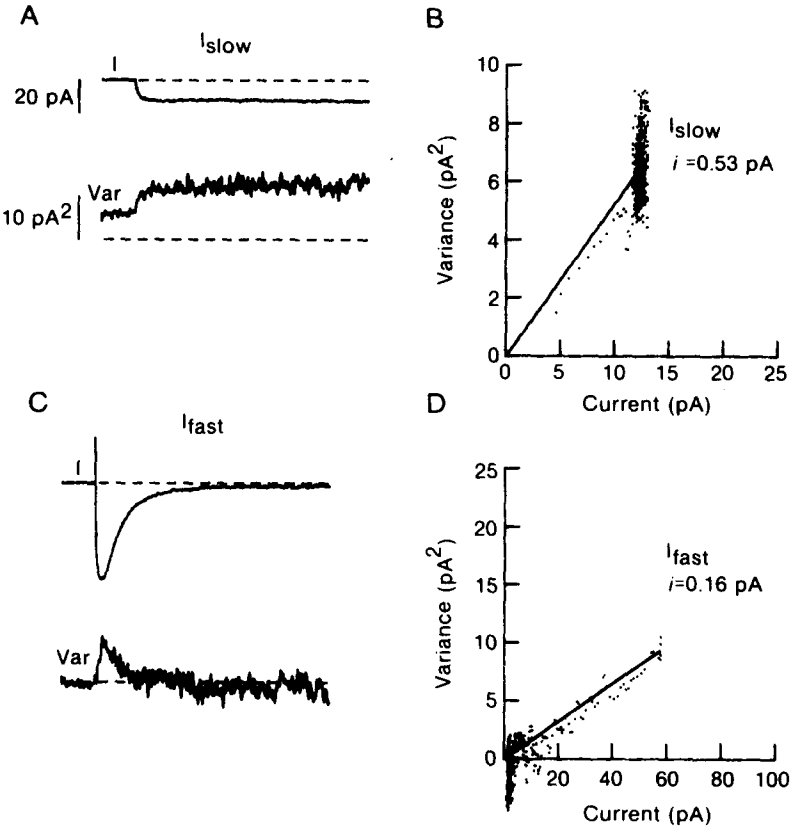

FIGURE 12. Isolation of mean current and variance for I_{fast} and I_{slow}. (*A*) Mean I_{slow} (trace labeled −40 in Fig. 11) and variance. (*B*) Variance-mean plot fit by theory for a population of homogeneous, independently gated channels (see text). Before plotting, background variance (measured at the holding potential) was subtracted from the variance trace. (*C*) Mean I_{fast} and variance from I_{fast}, isolated by subtraction of the traces in Fig. 11. (*D*) Variance-mean scattergram and fit by theory. Data from the rising phase of the current are omitted from the plot to avoid contamination by the outward transient.

current and variance arising from the fast component of current, isolated by subtraction. Again, the relationship is nearly linear, which suggests that p_{max} is low for this current as well. However, the value of i obtained from the theoretical fit, 0.16 pA, is considerably smaller than that for the slow component at the same test potential. The results in this cell were typical; in the collected results from cells under identical conditions, i at −10 mV was 0.21 ± 0.04 pA ($N = 4$)

for I_{fast} and 0.58 ± 0.06 pA (N = 6) for I_{slow}. Fig. 13 shows the collected results of measurements of i at various membrane potentials (below −20 mV, where activation of I_{slow} was negligible, i for I_{slow} was estimated from tail currents following stronger activating depolarizations). The results show that over the range it could be measured, −30 to −10 mV, i for I_{fast} was much lower than i for I_{slow}. The values of i for each current can be tolerably fit by a curve drawn

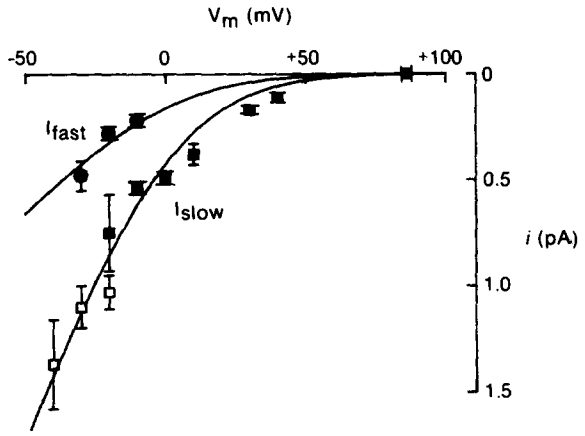

FIGURE 13. Collected i values from fluctuation analysis of I_{fast} and I_{slow}. Points are means ± SEM for 3–11 determinations at each potential. For I_{slow}, closed symbols show values obtained from test pulses delivered from −40 mV, while open symbols show values from analysis of tail currents following prepulses to 0 to +40 mV. In tail current analysis, only the last third of the tail was used to ensure clear separation from the capacity current and to avoid possible series resistance errors from large initial tail currents. Tail currents followed activating pulses elicited from −40 mV, so that only I_{slow} was present in the tail. The square on the current axis is at +86 mV (±2 mV), the mean reversal potential measured for I_{slow} in 115 mM Ba (six cells). Values for I_{fast} were determined as in Fig. 11, with mean current and variance for a series from −40 mV subtracted from mean current and variance for another series from −80 mV. Solid lines show fits by constant field theory: $I = -4P_{Ba}(EF^2/RT) \cdot [Ba]_o \exp(-2EF/RT)/[1 - \exp(-2EF/RT)] + P_{Cs}(EF^2/RT)[Cs]_i/[1 - \exp(-EF/RT)]$. Constrained to give zero current at the reversal potential at +86 mV, the fit to the I_{slow} points was drawn with $P_{Ba} = 1.94 \times 10^{-14}$ cm³/s and $P_{Cs} = 0.0061 \times 10^{-14}$ cm³/s (with $[Ba]_o$ = 115 mM and $[Cs]_i$ = 145 mM). Reversal potentials for I_{fast} could not be accurately determined but were within 10–20 mV of those for I_{slow}. For convenience, the reversal potential for I_{fast} is also assumed to be +86 mV and the fit is drawn according to $P_{Ba} = 0.73 \times 10^{-14}$ cm³/s and $P_{Cs} = 0.0023 \times 10^{-14}$ cm³/s.

according to constant field theory for a divalent:monovalent situation (Fatt and Ginsborg, 1958). (The fits should be regarded as no more than an empirically useful way of summarizing the data, since it is already very clear [cf. Hess and Tsien, 1984] that the assumption of independent ion movement underlying the constant field theory does not apply, at least in the slow Ca channel.) From the fitted curves, the Ba permeability of a single channel of the slow type is 1.94×10^{-14} cm³/s; the Ba permeability of a single fast channel is more than two times

smaller, 0.73×10^{-14} cm^3/s. (These figures lump the Ba activity coefficient into the permeability and assume no difference between internal and external surface potentials; the latter seems a reasonable assumption under these ionic conditions [cf. Lee and Tsien, 1984].)

These results, taken together with the different degrees of discrimination between Ca and Ba, provide a strong indication that the open channel properties, and the details of ion permeation, are different for the two kinds of channels. The data in Figs. 11 and 12 provide fairly conclusive evidence against the possibility that the two components of current merely represent the complicated kinetic behavior of a single kind of channel. This hypothesis would require that the variance:mean current ratio be similar for both components of current, while it is actually different by a factor of almost 3.

For large depolarizations, there was enough curvature in the variance-mean current plots for I_{slow} to estimate the number of slow channels in a cell; at +30 mV, p_{max} was 0.18 ± 0.03 (N = 7) and N was 27,100 ± 3,900 (assuming 1 μF/cm^2, this corresponds to a channel density of about four channels per square micron). However, even for the largest depolarizations for which I_{fast} could be analyzed, at −10 mV, p_{max} was too low to allow an accurate estimate of N. This leaves open the possibility that the numbers of the two channel types per cell could be similar, even though the maximal current carried by I_{slow} is usually much larger.

Block by Nitrendipine

The dihydropyridine drugs are the most potent blockers of cardiac Ca currents. Since the binding of tritiated derivatives is widely used to estimate Ca channel density and as an aid to biochemical purification of Ca channels, it is interesting to know whether both kinds of channels can be blocked by dihydropyridines. The experiment shown in Fig. 14 examined the susceptibility of the two currents to block by nitrendipine. Fig. 14*A* shows the effect of 3 μM nitrendipine on I_{slow} (elicited in isolation from −30 mV) near the peak of the *I-V* curve; peak current was blocked to ~30% of control, in rough agreement with previous studies in ventricular cells using similar protocols (Lee and Tsien, 1983; Sanguinetti and Kass, 1984*a*; Bean, 1984). Fig. 14*B* shows the effect of nitrendipine (in the same application) on current elicited from a step from −80 to −10 mV, where peak current is mainly due to I_{fast}; peak current is unchanged by nitrendipine, which suggests little block of I_{fast}. Surprisingly, however, nitrendipine actually *increased* the current late in the pulse. Since this steady current is due to I_{slow}, it appears that nitrendipine increases I_{slow} for small depolarizations. This effect is seen clearly in Fig. 14*C*, where I_{slow} at 0 mV was elicited in isolation by a depolarization from −30 mV; nitrendipine increased the current by a factor of >2 (for the same application that decreased I_{slow} at +30 mV by a factor of 3). Hess et al. (1984) have recently noted that nitrendipine can cause changes in single channel kinetics like those produced by the so-called "Ca agonist" BAY K8644 (although the net effect of nitrendipine was inhibitory in their experiments). The experiment in Fig. 14 provides direct confirmation that nitrendipine, usually thought of as a blocker, can also act as a "Ca agonist," and shows that at some potentials, this

effect can predominate. Similar effects have recently been reported by Brown et al. (1985). The effect in Fig. 14, *B* and *C*, could very well underlie the increase in contractility sometimes seen in vascular smooth muscle treated with nitrendipine.

Fig. 14*D* shows the effect of nitrendipine on I_{fast} isolated by the usual subtraction procedure. With the potentiation of I_{slow} removed, the records show that 3 μM nitrendipine produced a very small (15%) decrease in peak I_{fast} and perhaps a slight speeding of its decay.

These results were typical of other experiments with nitrendipine: 1 μM nitrendipine always reduced I_{slow} by a factor of >2, but had no effect on I_{fast}; 3 μM nitrendipine reduced I_{slow} by a factor of ≥3, while reducing I_{fast} by only 10–

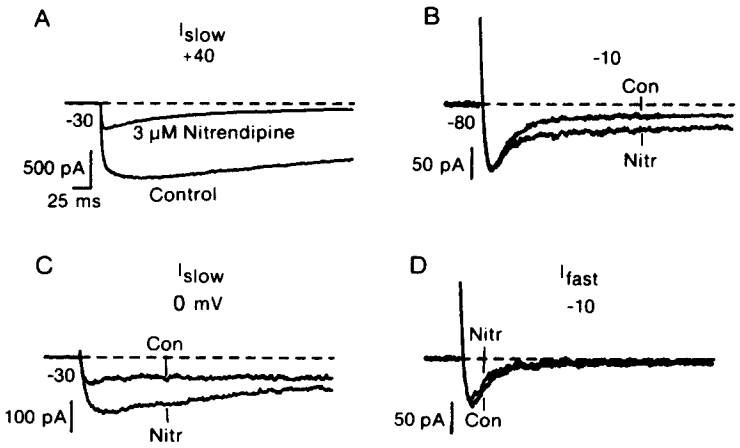

FIGURE 14. Block of I_{fast} and I_{slow} by 3 μM nitrendipine. (*A*) Block of I_{slow} at +40 mV; the trace labeled "nitrendipine" was recorded 1 min after superfusion with nitrendipine-containing solution. (*B*) Effect of nitrendipine on total current elicited by pulse to −10 mV from −80 (same application of nitrendipine as in *A*). (*C*) Effect of nitrendipine on I_{slow} elicited at 0 mV from a holding potential of −30 mV (same application). (*D*) I_{fast} (same data as in *B* but with I_{slow} subtracted). Filtered at 0.5 kHz. 115 mM Ba, 10 μM TTX. 77 pF. Cell B28F.

20%; 10 μM nitrendipine reduced I_{slow} by ~80% and reduced I_{fast} by ~50%. In three of three experiments with 3 μM nitrendipine, I_{slow} at −10 or 0 mV was increased, as in Fig. 14.

It has recently been found that dihydropyridine block of slow Ca current can be profoundly modulated by holding potential, producing large negative shifts in the inactivation curve (Sanguinetti and Kass, 1984*a*; Uehara and Hume, 1984). Just as for local anesthetic block of Na channels, the data can be interpreted by a modulated-receptor model (Hille, 1977; Hondeghem and Katzung, 1977), which hypothesizes tight binding to inactivated channels and weak binding to resting channels, and the K_d of 0.25 mM derived for binding to inactivated channels (Bean, 1984) is the same as measured for high-affinity binding of radiolabeled nitrendipine. On the modulated-receptor interpretation,

the block seen in experiments like that in Fig. 14 is primarily due to binding to resting channels. The possibility that nitrendipine might bind tightly to I_{fast} channels in the inactivated state was tested by looking for shifts in the inactivation curve; with the application of 1 μM nitrendipine, the inactivation curve for I_{fast} shifted only slightly (with a midpoint of −44.6 mV in control and a midpoint of −47.6 mV in nitrendipine). (The same application of nitrendipine shifted I_{slow} inactivation dramatically; measured at +40 mV, the ratio of current elicited from −30 to that from −80 changed from 0.96 in control to 0.42 in nitrendipine.) It thus seems likely that nitrendipine binding to the inactivated state of the fast channel is as weak, or nearly so, as to the resting state.

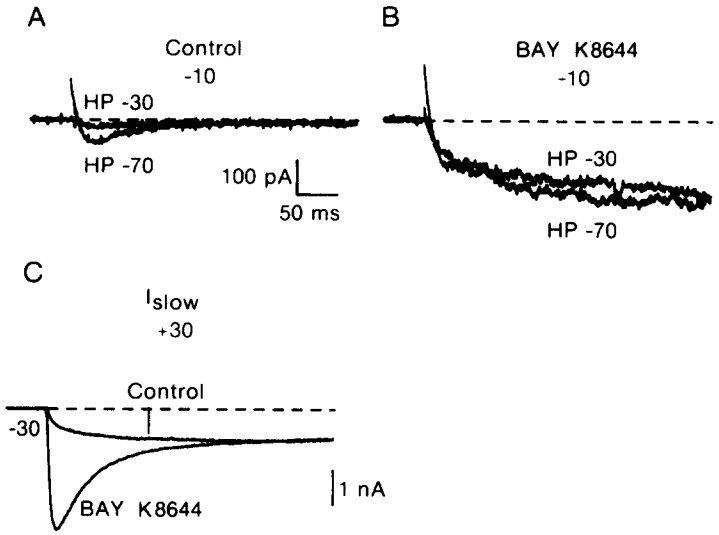

FIGURE 15. Effect of 500 mM BAY K8644 on Ca channel currents. (*A*) Control currents at −10 mV elicited from −30 or −70 mV. (*B*) 5 min after addition of BAY K8644 to superfusing solution. (*C*) Effect (in same application) on I_{slow} elicited at +30 mV from −30 mV. Filtered at 5 kHz. 115 mM Ba, no TTX. Cell B16L.

Potentiation by BAY K8644

Further evidence for the pharmacological dissimilarity of the two kinds of channels comes from an experiment with BAY K8644, a dihydropyridine that has recently been demonstrated to produce sizeable increases of Ca channel current (Kokubun and Reuter, 1984; Hess et al., 1984; Brown et al., 1984; Sanguinetti and Kass, 1984*b*). As shown in Fig. 15, this drug increased the I_{slow} component of current but had no obvious effect on I_{fast}. I_{slow} was increased at all voltages. (The increase in I_{slow} at −10 mV was so large that it was impossible to isolate I_{fast} accurately with drug present, but there was clearly no increase in I_{fast} as large as that in I_{slow}.) The result is consistent with the nitrendipine experiments in suggesting that I_{fast} channels are much less insensitive to dihydropyridines.

Effect of Isoproterenol

The stimulation of β-adrenergic receptors by adrenaline or isoproterenol increases cardiac Ca current (Reuter, 1967, 1983; Tsien, 1983). Fig. 16 shows the effect of 4 μM isoproterenol on a cell bathed in isotonic $BaCl_2$. Isoproterenol increased I_{slow}, elicited by a pulse from −30 to +30 mV, by a factor of ~2. The increase in current is accompanied by a dramatic slowing of the activation kinetics, as seen in other kinds of cells under similar conditions (Bean et al., 1984). However, as shown in Fig. 16*B*, isoproterenol in the same application

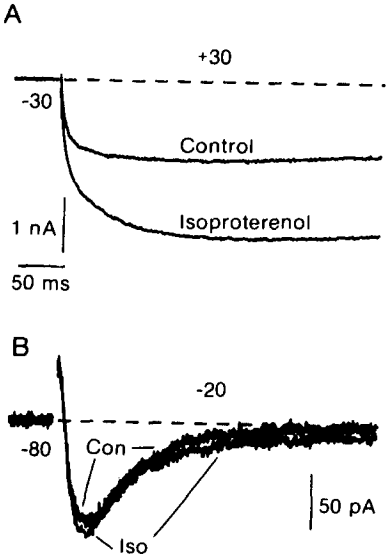

FIGURE 16. Effect of isoproterenol stimulation. 115 mM Ba, no TTX. (*A*) Increase of I_{slow} by 4 μM isoproterenol. The larger current was recorded 4 min after superfusion with isoproterenol solution. (*B*) Effect on current for −80 to −20 mV step, for same application of isoproterenol. Traces are the average of four sweeps in each case. Leak and capacity corrected. Cell B16D.

had almost no effect on current elicited by a step from −80 to −20 mV (almost purely I_{fast}). The only effect was a very small increase in current both near the peak and in the steady state, which is consistent with an augmentation of a small component of I_{slow} at this potential. The same results were obtained in each of four cells; 4 μM isoproterenol increased current at +30 mV (all or nearly all I_{slow}) by a factor of 2 (average increase 116 ± 3%), but peak current at −20 or −10 mV (almost pure I_{fast}) was increased insignificantly, by 6 ± 6%. Thus, I_{fast} channels, unlike I_{slow} channels, are not regulated by β-receptor stimulation.

DISCUSSION

The principal new finding of this study is evidence for the existence of two distinct populations of Ca channels in atrial cells. The two components of current

that can be distinguished kinetically have different selectivity between Ca and Ba, different single channel currents, different sensitivity to dihydropyridine drugs, and different sensitivity to β-adrenergic stimulation. Taken together, these findings constitute strong evidence that the two components actually arise from two different kinds of Ca channels.

The slow Ca channel in canine atrial cells seems likely to be identical to the Ca channels described in single mammalian ventricular cells in recent years. Thus, the voltage dependence of activation and inactivation, larger current amplitudes with Ba than with Ca, β-adrenergic augmentation of current, and the potency of nitrendipine block are all similar to results with various ventricular cells (Isenberg and Klockner, 1982; Lee and Tsien, 1982; Mitchell et al., 1983; Hess and Tsien, 1984; Lee and Tsien, 1984). The kinetics of inactivation in Ca-containing solutions are slower in the currents presented here than in published records from ventricular cells voltage-clamped with one or two microelectrodes (Isenberg and Klockner, 1982; Mitchell et al., 1983; Josephson et al., 1984), but this is undoubtedly due to the presence of internal EGTA, which slows inactivation considerably.

It is not necessarily surprising that the fast Ca channel has not been observed before in heart cells. In Na-containing solutions, the fast Ca current is obscured by Na current if negative holding potentials are used, and it is likely to be inactivated at the positive holding potentials frequently used to inactivate Na current (although there is a narrow band of holding potentials at which Na current is inactivated while fast Ca current is not). Also, although the inactivation kinetics of I_{fast} and I_{slow} are very different in Ba solutions (Fig. 2), they are not so different in Ca solutions (Fig. 4) and might be even more similar in the absence of internal EGTA.

Other kinds of cardiac cells may have even more prominent components of fast Ca current. In several preliminary experiments with bullfrog atrial cells isolated as described by Hume and Giles (1981, 1983), I have seen both components of Ca channel current, with I_{fast} two to three times larger than I_{slow} in some cells. Also, several experiments with spontaneously beating cells isolated from the sinoatrial node of dog hearts showed the presence of both components of current, with similar magnitudes as in atrial cells. It will be interesting to explore the distribution of the two kinds of channels in various regions of the heart in more detail; already, experiments suggest that there is no systematic difference in the magnitude of the two currents in different regions of the right atrium but, as already mentioned, ventricular cells have much less I_{fast} and more I_{slow}.

Lee et al. (1984; see also Nobel, 1984) have recently suggested that in guinea pig ventricular cells, there is, in addition to the usual slow Ca current, a very slow Ca current that can be distinguished by its lesser sensitivity to Cd block. Since this current obviously does not correspond to either of the Ca channels reported here for atrial cells, there may well be (at least) three distinct kinds of cardiac Ca channels.

Comparison with the Inactivating Ca Channels in Other Cells

The fast channel in atrial cells seems very similar to the fast-inactivating Ca channel recently discovered in neurons. Just as for the fast atrial channel (Fig.

5), the fast neuronal Ca channel in 5 mM Ca first activates at about −50 mV and produces a peak current at −30 mV (Carbone and Lux, 1984*a*). The kinetics are also very similar, with peaks occurring at 10–20 ms and inactivation time constants of 50–10 ms; also, in both channels, inactivation is faster with larger depolarizations and the kinetics are much the same in Ca and Ba solutions (Nowycky et al., 1984*a*; Carbone and Lux, 1984*a*). The only obvious difference is that the neuronal channel has an inactivation curve with a midpoint at −80 mV (Carbone and Lux, 1984*a*; Fedulova et al., 1985), to the left of the Na channel inactivation curve, while the heart channel has a midpoint near −50 mV in 5–20 mM Ca, to the right of the Na channel inactivation curve.

There are also similarities to inactivating Ca channels in other kinds of cells. The Ca current studied in N1E-115 neuroblastoma cells by Moolenaar and Spector (1979) is very similar to the fast current in atrial cells in its kinetics, placement of inactivation curve, and lack of discrimination between Ca and Ba. Tsunoo et al. (1984) found that a slow, nonactivating component of current in the same neuroblastoma cells was increased by dibutyryl cyclic AMP, but that the fast-inactivating component was not; these results fit well with the differential effect of isoproterenol observed with the atrial cells (Fig. 16). (Fedulova et al. [1985] have similarly reported that the fast-inactivating current in dorsal root ganglion cells is unaffected by cyclic AMP, which does regulate the slow current in the same cells.)

Armstrong and Matteson (1985) distinguished two types of Ca channels in cultured pituitary cells by differences in tail current kinetics; a fast-inactivating channel activated by low depolarizations had slow deactivation kinetics, while a slowly inactivating channel had fast deactivation kinetics. Similarly, in the present series of experiments, I found that the fast-inactivating channel in cardiac cells has much slower tail currents than the slowly inactivating channel, although a complete study of tail kinetics has not yet been made. In another line of cultured pituitary cells, Cohen and McCarthy (1985) found that a slowly inactivating component of Ca current was eliminated by the dihydropyridine drug nimodipine, while a fast-inactivating component was unaffected; these results are very similar to those for nitrendipine effects on the two Ca currents in atrial cells. (Miller [1985] reviews other experiments that suggest the existence of both dihydropyridine-sensitive and -insensitive Ca channels in various neuronal cell types.)

All of the fast-inactivating Ca currents reported recently seem kinetically similar to the fast-inactivating Ca current described in polychaete eggs (Fox, 1981; Fox and Krasne, 1984); the observation that fast channel inactivation in atrial cells is unaffected by exchanging Ca for Ba (Fig. 10) matches Fox's (1981) result closely.

Mechanism of Fast Channel Inactivation

The mechanism of fast channel inactivation is not yet completely clear. The rapidity of inactivation with high internal EGTA, as well as the lack of effect when Ba replaces Ca, makes a purely Ca-dependent mechanism seem unlikely (see Eckert and Chad, 1984). However, since all the experiments were done with EGTA, the possibility remains that native inactivation could be even faster if an

additional contribution of Ca-dependent inactivation were eliminated by EGTA. Another possibility is that inactivation represents ion depletion, as for example might occur if the fast channels were preferentially located in caveolae with small volumes. However, depletion seems unlikely to be the primary mechanism since changes in external ion concentration have little effect on inactivation kinetics. Currents in 115 mM Ba or 5 mM Ca decay at about the same rate (compare Figs. 2 and 4), and in other experiments, changing the concentration of a single ion species had little effect on inactivation kinetics. Taken together, the present data are most simply explained by a Na channel–like, voltage-dependent inactivation mechanism, although other mechanisms are not completely ruled out and many questions remain, including the kinetic relationship of the inactivation mechanism to the activation process.

Permeation Properties

Most recordings of single Ca channels in ventricular myocytes (Reuter et al., 1982; Cavalie et al., 1983; Hess et al., 1984) have shown open channel properties similar to those in neurons and other cells (Fenwick et al., 1982; Hagiwara and Ohmori, 1983; Lux and Brown, 1984). With modest depolarizations, the single channel current is ~1 pA in isotonic $BaCl_2$, and the single channel conductance is 10–25 pS. The slow channel observed in the atrial cells fits well with these earlier results, both from the single channel currents derived from fluctuation analysis (Fig. 13) and from direct recordings of single channel currents, which give results very similar to those in Fig. 13, assuming reasonable values for cell resting potential (unpublished results). There is an apparent difference between the results in Fig. 13 and previous fluctuation analysis estimates of single channel current in chromaffin (Fenwick et al., 1982) and pituitary (Hagiwara and Ohmori, 1982) cells. Both these previous studies observed saturation of i values below 0 mV instead of the superlinearity seen in Fig. 13. However, this may simply be due to the fact that the data in Fig. 13 have been extended to more negative potentials by using tail currents to analyze currents at −40 to −20 mV. (Another possibility is that the small amounts of Na or K used to titrate the $BaCl_2$ solutions used in the previous studies could induce partial block at negative potentials.) Since superlinearity like that in Fig. 13 was also seen directly with single channel recording in the canine atrial cells, it is unlikely to be due to an overestimate of i at negative potentials.

The fast channel in atrial cells has single channel currents in 115 mM Ba that are less than half of those of the slow channel. This seems to fit well with the observation that the fast-inactivating channel in dorsal root ganglion cells has a different single channel current than the "slow" channel in the same cells, with unitary currents from inactivating channels considerably smaller in 110 mM Ba (Nowycky et al., 1984*b*). However, Carbone and Lux (1984*b*) found that in 20 mM Ca, the fast-inactivating channel has a *larger* unitary current than the slow channel. Given the different selectivity between Ca and Ba shown by the fast and slow channels in atrial cells, these results are not necessarily inconsistent with one another.

Because of the different permeability characteristics of the two kinds of

channels, it would not be unexpected to find different block by inorganic ions, since it is likely that the same binding sites that govern permeation by Ca and Ba also govern block by other divalents (Hagiwara and Byerly, 1981; Hess and Tsien, 1984; Almers and McCleskey, 1984). In the present study, Co was equally effective in blocking current through both channels. However, 2 mM Mn was found to block I_{slow} by ~70%, while leaving I_{fast} untouched. Similarly, Nowycky et al. (1984*b*) found that the inactivating current in dorsal root ganglion cells was less sensitive to Cd block than the long-lasting current. In heart and skeletal muscle channels corresponding to the slow Ca channel in atrial cells, it has been found that Ca itself can block current through the channel, either in micromolar concentrations when current is carried by Na or other monovalent ions or in millimolar concentrations when current is carried by Ba (Almers et al., 1984; Hess and Tsien, 1984). These findings, as well as the selectivity between Ca and Ba and saturation phenomena, can be elegantly explained by a two-binding-site model of the channel permeation pathway (Hess and Tsien, 1984; Almers and McCleskey, 1984). It will be interesting to see if the fast Ca channel is blocked in a similar way by Ca and if all Ca channels have the same basic selectivity mechanism. Already, experiments on I_{fast} in atrial cells show that peak current saturates at high Ca (results not shown), and similar findings can be seen in the records from neurons (Carbone and Lux, 1984*a*; Fedulova et al., 1985).

Nitrendipine Block and High-Affinity Binding Sites

The results show that fast channels are relatively insensitive to block by nitrendipine (or augmentation by BAY K8644). Nitrendipine block of slow channels is complicated. Adding to the previously observed voltage-dependent block (Sanguinetti and Kass, 1984*a*; Uehara and Hume, 1984; Bean, 1984) is the agonist-like effect of nitrendipine on channel kinetics (Hess et al., 1984), which, as shown in Fig. 14, can actually produce net augmentation of macroscopic currents under some circumstances (see also Brown et al., 1985). How the various effects depend on test potential, and how they relate to radiolabel binding sites on the channel, remains to be worked out. Although the kinetics and affinity of radiolabel binding to the high-affinity site match very well with electrophysiological determinations of binding to inactivated channels (Bean, 1984), it seems that accounting for both agonist and antagonist effects of nitrendipine (Hess et al., 1984; Brown et al., 1985) and BAY K8644 (Sanguinetti and Kass, 1984*b*) will require complicated models, perhaps invoking multiple binding sites. In contrast, it seems likely that there is no high-affinity binding at all to fast Ca channels: the K_d for block from negative potentials is ~10 μM, and since there is little, if any, enhancement of block at holding potentials that inactivate channels, binding to inactivated fast channels is probably almost as weak. Fast channels will probably not be purified by biochemical procedures that rely on dihydropyridine binding. It will be interesting to see if the differences between slow and fast channels extend to other blockers like verapamil and diltiazem, which are used as antiarrhythmic agents and which bind to different sites than dihydropyridines. In both dorsal root ganglion cells (Fedulova et al., 1985) and neuroblastoma cells (Tsunoo et al., 1985), the fast-inactivating channel seems less sensitive to verapamil than

the slow channel. Differences in the pharmacology of fast and slow channels in cardiac muscle are obviously of great interest for understanding the clinical pharmacology of Ca blocker drugs.

Functional Significance of Fast Ca Channels

It is not clear whether the existence of the fast Ca channels has some special significance for the function of atrial cells. Under normal circumstances, current through the channels is unlikely to be very important for electrical excitability since, in a well-polarized atrial cell, Na current is much larger and activates in a similar voltage range. Also, to the extent that the slow Ca channels inactivate more slowly, they are likely to be more important than fast channels for maintaining the action potential plateau. There is more room for the electrical importance of fast Ca channels in cells that are more depolarized, including sinoatrial and atrioventricular cells, or ischemic, partially depolarized atrial cells. Since the inactivation curve for Na channels is ~10 mV more hyperpolarized than for that for I_{fast}, there is a band of resting potentials (−65 to −55 in normal Tyrode's) where I_{fast} channels are available but Na channels are not. Fast Ca channels would be useful in cells capable of spontaneous activity, since they will be activated at relatively negative potentials and will help depolarize the cell but will then inactivate quickly, helping prevent excessively long plateaus. The low threshold of the fast channels could also make them especially useful for the propagation of the atrioventricular nodal Ca action potential.

In some cells (e.g., the one in Figs. 4 and 5), Ca entry through fast channels could be a sizeable fraction of total Ca entry. However, in most cells, current through slow channels is quite a bit larger, especially at the positive potentials that an atrial action potential quickly reaches, so it is not obvious that there is any special advantage of the presence of fast channels for initiation of contractile activation or triggering Ca release from the sarcoplasmic reticulum.

An especially intriguing feature of the fast channels is that the probability of opening is so low, as revealed by the fluctuation analysis experiments. Even at −10 mV in 115 mM Ba, near the peak of the *I-V* curve, p_{max} is very low (<0.2). This leaves open the possibility that current through the channels could be increased manyfold through an increase in the probability of opening, perhaps through channel modulation by neurotransmitters, hormones, second messengers, or drugs. Although β-adrenergic stimulation, which does increase p_{max} for slow channels via a cAMP mechanism (Cachelin et al., 1983; Brum et al., 1984; Bean et al., 1984), had no effect on I_{fast}, there are many other neurotransmitters and hormones that have been shown to modulate overall Ca current or Ca-dependent action potentials. It will be interesting to see whether fast channels can be controlled by acetylcholine, angiotensin, α-adrenergic stimulation, or opioid peptides.

I am grateful to Phil Karp, Tim Ruppert, and Dr. Mike Welsh for assistance in obtaining hearts, and to Drs. Kurt Beam and Kevin Campbell for helpful discussion.
This work was supported by National Institutes of Health grant HL 32663.

Original version received 2 January 1985 and accepted version received 27 March 1985.

REFERENCES

Almers, W., and E. W. McCleskey. 1984. Non-selective conductance in calcium channels of frog muscle: calcium selectivity in a single-file pore. *J. Physiol. (Lond.).* 353:585–608.

Almers, W., E. W. McCleskey, and P. T. Palade. 1984. A non-selective cation conductance in frog muscle membrane blocked by micromolar external calcium ions. *J. Physiol. (Lond.).* 353:565–583.

Armstrong, C. M., and D. R. Matteson. 1985. Two distinct populations of calcium channels in a clonal line of pituitary cells. *Science (Wash. DC).* 277:65–67.

Bean, B. P. 1984. Nitrendipine block of cardiac calcium channels: high-affinity binding to the inactivated state. *Proc. Natl. Acad. Sci. USA.* 81:6388–6392.

Bean, B. P. 1985. Two kinds of calcium channels in atrial cells from dog and frog hearts. *Biophys. J.* 47:497*a*. (Abstr.)

Bean, B. P., M. C. Nowycky, and R. W. Tsien. 1984. Beta-adrenergic modulation of calcium channels in frog ventricular heart cells. *Nature (Lond.).* 307:371–375.

Brown, A. M., D. L. Kunze, and A. Yatani. 1984. The agonist effect of dihydropyridines on Ca channels. *Nature (Lond.).* 311:570–572.

Brown, A. M., D. L. Kunze, and A. Yatani. 1985. Agonist effect of a dihydropyridine Ca channel blocker on guinea pig and rat ventricular myocytes. *J. Physiol. (Lond.).* 357:59*p*. (Abstr.)

Brum, G., W. Osterreider, and W. Trautwein. 1984. Beta-adrenergic increase in the calcium conductance of cardiac myocytes studied with the patch clamp. *Pflügers Arch. Eur. J. Physiol.* 401:111–118.

Bustamente, J. O., T. Watanabe, D. A. Murphy, and T. F. McDonald. 1982. Isolation of single atrial and ventricular cells from the human heart. *Can. Med. Ass. J.* 126:791–793.

Cachelin, A. B., J. E. DePeyer, S. Kokubun, and H. Reuter. 1983. Calcium channel modulation by 8-bromo-cyclic AMP in cultured heart cells. *Nature (Lond.).* 304:462–464.

Carbone, E., and H. D. Lux. 1984*a*. A low voltage-activated calcium conductance in embryonic chick sensory neurons. *Biophys. J.* 46:413–418.

Carbone, E., and H. D. Lux. 1984*b*. A low voltage-activated, fully inactivating Ca channel in vertebrate sensory neurones. *Nature (Lond.).* 310:501–502.

Cavalie, A., R. Ochi, D. Pelzer, and W. Trautwein. 1983. Elementary currents through Ca^{2+} channels in guinea pig myocytes. *Pflügers Arch. Eur. J. Physiol.* 398:284–297.

Cohen, C. J., B. P. Bean, T. J. Colatsky, and R. W. Tsien. 1981. Tetrodotoxin block of sodium channels in rabbit Purkinje fibrs. Interactions between toxin binding and channel gating. *J. Gen. Physiol.* 78:383–411.

Cohen, C. J., and R. T. McCarthy. 1985. Differential effects of dihydropyridines on two populations of Ca channels in anterior pituitary cells. *Biophys. J.* 47:513*a*. (Abstr.)

Conti, F., B. Hille, B. Neumcke, W. Nonner, and R. Stampfli. 1976. Measurement of the conductance of the sodium channel from current fluctuations at the node of Ranvier. *J. Physiol. (Lond.).* 262:699–727.

Corey, D. P., J. M. Dubinsky, and E. A. Schwartz. 1984. The calcium current in inner segments of rods from the salamander (*Ambystoma tigrinum*) retina. *J. Physiol. (Lond.).* 354:557–575.

Deitmer, J. W. 1984. Evidence for two voltage-dependent calcium currents in the membrane of the ciliate. *Stylonychia. J. Physiol. (Lond.).* 355:137–159.

Dubinsky, J. M., and G. S. Oxford. 1984. Ionic currents in two strains of rat anterior pituitary cells. *J. Gen. Physiol.* 83:309–339.

Eckert, R., and J. E. Chad. 1984. Inactivation of Ca channels. *Prog. Biophys. Mol. Biol.* 44:215–267.

Fatt, P., and B. L. Ginsborg. 1958. The ionic requirements for the production of action potentials in crustacean muscle fibres. *J. Physiol. (Lond.)*. 142:516–543.

Fedulova, S. A., P. G. Kostyuk, and N. S. Veselovsky. 1985. Two types of calcium channels in the somatic membrane of newborn rat dorsal root ganglion neurons. *J. Physiol. (Lond.)*. 359:431–446.

Fenwick, E. M., A. Marty, and E. Neher. 1982. Sodium and calcium channels in bovine chromaffin cells. *J. Physiol. (Lond.)*. 331:599–635.

Fox, A. P. 1981. Voltage dependent inactivation of a calcium channel. *Proc. Natl. Acad. Sci. USA*. 78:953–956.

Fox, A. P., and S. Krasne. 1984. Two calcium currents in *Neanthes arenaceodentatus* egg cell membranes. *J. Physiol. (Lond.)*. 356:491–505.

Hagiwara, S. 1983. Membrane Potential-dependent Ion Channels in Cell Membrane. Raven Press, New York. 5–59.

Hagiwara, S., and L. Byerly. 1981. Calcium channel. *Annu. Rev. Neurosci.* 4:69–125.

Hagiwara, S., and H. Ohmori. 1982. Studies of calcium channels in rat clonal pituitary cells with patch electrode voltage clamp. *J. Physiol. (Lond.)*. 331:231–252.

Hagiwara, S., and H. Ohmori. 1983. Studies of single calcium channel currents in rat clonal pituitary cells. *J. Physiol. (Lond.)*. 336:649–661.

Hagiwara, S., S. Ozawa, and O. Sand. 1975. Voltage clamp analysis of two inward current mechanisms in the egg cell membrane of a starfish. *J. Gen. Physiol.* 65:617–644.

Hamill, O. P., A. Marty, E. Neher, B. Sakmann, and F. J. Sigworth. 1981. Improved patch clamp techniques for high-resolution current recording from cells and cell-free membrane patches. *Pflügers Arch. Eur. J. Physiol.* 391:85–100.

Hess, P., J. B. Lansman, and R. W. Tsien. 1984. Different modes of Ca channel gating behaviour favoured by dihydropyridine Ca agonists and antagonists. *Nature (Lond.)*. 311:538–544.

Hess, P., and R. W. Tsien. 1984. Mechanism of ion permeation through calcium channels. *Nature (Lond.)*. 309:453–456.

Hille, B. 1977. Local anesthetics: hydrophilic and hydrophobic pathways for the drug:receptor reaction. *J. Gen. Physiol.* 69:497–515.

Hondeghem, L. M., and B. G. Katzung. 1977. Time- and voltage-dependent interactions of antiarrhythmic drugs with cardiac sodium channels. *Biochim. Biophys. Acta*. 472:373–398.

Hume, J. R., and W. Giles. 1981. Active and passive electrical properties of single bullfrog atrial cells. *J. Gen. Physiol.* 78:18–43.

Hume, J. R., and W. Giles. 1983. Ionic currents in single isolated bullfrog atrial cells. *J. Gen. Physiol.* 81:153–194.

Isenberg, G., and U. Klockner. 1982. Calcium currents of isolated ventricular myocytes are fast and of large amplitude. *Pflügers Arch. Eur. J. Physiol.* 395:30–41.

Josephson, I. R., J. Sanchez-Chapula, and A. M. Brown. 1984. A comparison of calcium currents in rat and guinea pig single ventricular cells. *Circ. Res.* 54:144–156.

Kokubun, S., and H. Reuter. 1984. Dihydropyridine derivatives prolong the open state of Ca channels in cultured cardiac cells. *Proc. Natl. Acad. Sci. USA*. 81:4824–4827.

Lee, K. S., D. Noble, E. Lee, and A. J. Spindler. 1984. A new calcium current underlying the plateau of the cardiac action potential. *Proc. R. Soc. Lond. B Biol. Sci.* 223:35–48.

Lee, K. S., and R. W. Tsien. 1982. Reversal of current through calcium channels in dialysed single heart cells. *Nature (Lond.)*. 297:498–501.

Lee, K. S., and R. W. Tsien. 1983. Mechanism of calcium channel blockade by verapamil, D600, diltiazem and nitrendipine in single dialysed heart cells. *Nature (Lond.)*. 302:790–794.

Lee, K. S., and R. W. Tsien. 1984. The selectivity of calcium channels in single dialysed heart cells of the guinea pig. *J. Physiol. (Lond.).* 354:253–272.

Llinas, R., and Y. Yarom. 1981*a*. Electrophysiology of mammalian inferior olivary neurones *in vitro*. Different types of voltage-dependent ionic conductances. *J. Physiol. (Lond.).* 315:549–567.

Llinas, R., and Y. Yarom. 1981*b*. Properties and distribution of ionic conductances generating electroresponsiveness of mammalian inferior olivary neurones *in vitro*. *J. Physiol. (Lond.).* 315:569–584.

Lux, H. D., and A. M. Brown. 1984. Patch and whole cell calcium currents recorded simultaneously in snail neurons. *J. Gen. Physiol.* 83:727–750.

Marty, A., and E. Neher. 1983. Tight-seal whole-cell recording. *In* Single-Channel Recording. B. Sakmann and E. Neher, editors. Plenum Press, New York. 107–122.

Matteson, D. R., and C. M. Armstrong. 1984*a*. Evidence for two types of Ca channels in GH3 cells. *Biophys. J.* 45:36*a*. (Abstr.)

Matteson, D. R., and C. M. Armstrong. 1984*b*. Na and Ca channels in a transformed line of anterior pituitary cells. *J. Gen. Physiol.* 83:371–394.

Miller, R. J. 1985. How many types of calcium channels exist in neurones? *Trends Neurosci.* 8:45–47.

Mitchell, M. R., T. Powell, D. A. Terrar, and V. W. Twist. 1983. Characteristics of the second inward current in cells isolated from rat ventricular muscle. *Proc. R. Soc. Lond. B Biol. Sci.* 219:447–469.

Moolenaar, W. H., and I. Spector. 1979. The calcium current and the activation of a slow potassium conductance in voltage-clamped mouse neuroblastoma cells. *J. Physiol. (Lond.).* 292:307–323.

Noble, D. 1984. The surprising heart: a review of recent progress in cardiac electrophysiology. *J. Physiol. (Lond.).* 351:1–50.

Nowycky, M. C., A. P. Fox, and R. W. Tsien. 1984*a*. Two components of calcium channel current in chick dorsal root ganglion cells. *Biophys. J.* 45:36*a*. (Abstr.)

Nowycky, M. C., A. P. Fox, and R. W. Tsien. 1984*b*. Multiple types of calcium channels in dorsal root ganglion cells distinguished by sensitivity to cadmium and single channel properties. *Soc. Neurosci.* 10:526. (Abstr.)

Reuter, H. 1967. The dependence of the slow inward current on external calcium concentration in Purkinje fibres. *J. Physiol. (Lond.).* 192:479–492.

Reuter, H. 1983. Calcium channel modulation by neurotransmitters, enzymes, and drugs. *Nature (Lond.).* 301:569–574.

Reuter, H. 1984. Ion channels in cardiac cell membranes. *Annu. Rev. Physiol.* 46:473–484.

Reuter, H., C. F. Stevens, R. W. Tsien, and G. Yellen. 1982. Properties of single calcium channels in cardiac cell culture. *Nature (Lond.).* 297:501–504.

Sanguinetti, M. C., and R. S. Kass. 1984*a*. Voltage-dependent block of calcium channel current in the calf cardiac Purkinje fiber by dihydropyridine calcium channel antagonists. *Circ. Res.* 55:336–348.

Sanguinetti, M. C., and R. S. Kass. 1984*b*. Regulation of cardiac calcium channel current and contractile activity by the dihydropyridine BAY K8644 is voltage-dependent. *J. Mol. Cell. Cardiol.* 16:667–670.

Sigworth, F. J. 1980. The variance of sodium current fluctuations at the node of Ranvier. *J. Physiol. (Lond.).* 307:97–129.

Tsien, R. W. 1983. Calcium channels in excitable cell membranes. *Annu. Rev. Physiol.* 45:341–358.

Tsunoo, A., M. Yoshii, and T. Narahashi. 1984. Two types of calcium channels in neuroblastoma cells and their sensitivities to cyclic AMP. *Soc. Neurosci.* 10:527. (Abstr.)

Tsunoo, A., M. Yoshii, and T. Narahashi. 1985. Differential block of two types of calcium channels in neuroblastoma cells. *Biophys. J.* 47:433*a*. (Abstr.)

Uehara, A., and J. R. Hume. 1984. Interactions of organic Ca channel antagonists with Ca channels in isolated frog atrial cells: test of a modulated receptor hypothesis. *Biophys. J.* 45:50*a*. (Abstr.)

Yoshii, M., A. Tsunoo, and T. Narahashi. 1985. Different properties in two types of calcium channels in neuroblastoma cells. *Biophys. J.* 47:433*a*. (Abstr.)